I.J. Weinberg† and J.C. Sethares
Rome Air Development Center Hanscom AFB, MA 01731

ABSTRACT

The dispersion relation, radiation impedance and insertion loss by two terminal and microstrip models for forward and backward volume waves including a gap between YIG and transducer are obtained for the first time.

Introduction

We here obtain the dispersion relation, radiation impedance and insertion loss for forward and backward volume waves arising in multistrip magnetostatic transducers for a uniform current distribution. Included for consideration are the meander line and parallel grating, the presence of two ground planes simultaneously and the presence of an air gap between YIG surface and the microstrip lines (see Figure 1). Comparisons are made between insertion loss based on our two terminal model and insertion loss based on the microstrip model[1].

Dispersion Relation

As shown earlier[2],[3] we solve the boundary value problem consisting of Maxwell's equations, the gyrometric relation and the constitutive relations utilizing the Polder tensor. By considering the appriate continuity and boundary conditions at the region junctions and boundaries and by taking the magnetostatic approximation and assuming there are no variations of physical quantities in the z direction (see Figure 1), we obtain a solution in the form of a magnetostatic potential function.

In non YIG regions the function is of the form

$$\psi = (Ae^{|k|y} + Be^{|k|y})e^{-ikx}e^{i\omega t} \qquad (1a)$$

and in the YIG region the function is of the form

$$\psi = (A\cos\alpha|k|y + B\sin\alpha|k|y)e^{-ikx}e^{i\omega t} \qquad (1b)$$

where

$$\alpha^2 = -\left(1 + \frac{\gamma^2 H_o M_o}{\gamma^2 H_o{}^2 - f^2}\right)^* \qquad (2)$$

where *=1 for forward waves and *=-1 for backward waves. Also, H_o is the biasing field magnitude, γ =2.8 mhz/oe, M_o = 1750 oe and f = $\omega/2$.

The determination of the A and B constants in (1) and (2) obtained by solving the boundary value problem leads to the dispersion relation in the form F(k) = 0 from which we find wave number k as a function of frequency from

$$|k| = \frac{1}{\alpha d}\tan^{-1}\left\{2\alpha\left[e^{|k|(t_1+g)} - e^{-2|k|\ell}e^{-|k|(t_1+g)}\right]\Big/\left[(\alpha^2-1)e^{|k|(t_1+g)} + (-1)^*(\alpha^2+1)e^{-|k|(t_1+g)} + (-1)^*e^{-2|k|\ell}(\alpha^2+1)e^{+|k|(t_1+g)} + e^{-2|k|\ell}(\alpha^2-1)e^{-|k|(t_1+g)}\right]\right\} \qquad (3)$$

†On leave from University of Lowell, Lowell, MA 01854.
Supported by AFOSR University Resident Research Program.

where t_1, g, d and l are the region thicknesses (see Figure 1) and here, *=0 for forward waves and *=1 for backward waves. Equation (3) is solved numerically by successive approximations. The principal value of the inverse tangent function is taken from 0 to π. An infinite number of solution modes of (3) can be found by considering the multiplicity of the inverse tangent function. Note that the solution waves are the same for positive and negative k for each solution mode. It is also seen that (3) reduces to expressions obtained earlier[4] when the gap g is reduced to 0.

Radiation Impedance

Upon satisfying the dispersion relation we find all constants in (1) as in earlier analysis[2],[3]. The field equations for h_x and b_y for all regions are found from (1) and the Polder tensor with Fourier transform analysis and contour integration. We then obtain the magnetostatic wave power for positive and negative k for each solution mode of (3). The fundamental mode contains most of the contribution to the power as is expected. The radiation resistance for positive and negative k are also identical and the total radiation resistance is twice the resistance from each wave, for every mode. The total resistance for each mode is then of the form

$$R_m = \frac{2\omega\mu_o|G|^2\,\ell_1}{k^2[(1-\eta)+(1+\eta)N^2]}\,C \qquad (4)$$

where

$$G = \frac{e^{-|k|d}\,\tilde{J}(k)}{\left|\frac{\partial}{\partial k'}F(k')\right|_{k'=k}} \qquad (5)$$

where C is obtained separately for forward waves and backward waves by integrating through the thickness for all regions.

$$C = 2e^{-2k\ell}(\sinh 2k\ell - 2k\ell) - 1 + (-1^*)(\alpha^2+1)kd - (-1)^*kg\left\{\frac{1+\alpha^2}{\alpha}\sin 2\alpha kd + \frac{1-\alpha^4}{2\alpha^2} - \frac{1-\alpha^4}{2\alpha^2}\cos 2\alpha kd\right)$$

$$+ (-1)^*\left(\frac{\sinh 2kt_1 - 2kt_1}{2\sinh^2 kt_1}\right)\left(\frac{\alpha^4-1}{4\alpha^2} - \frac{\alpha^4-1}{4\alpha^2}\cos 2\alpha kd - \frac{\alpha^2+1}{2\alpha}\sin 2\alpha kd\right)$$

$$+ e^{2k\ell}\left[\frac{(1+\alpha^2)^2}{8\alpha^2} + \frac{4\alpha^2-(1-\alpha^2)^2}{8\alpha^2}\cos 2\alpha kd + \frac{1-\alpha^2}{2\alpha}\sin 2\alpha kd\right]\left(1 + \frac{\sinh^2 2kt_1 - 2kt_1}{2\sinh^2 kt_1}\right)$$

$$+ e^{-2k\ell}\left[\frac{(1+\alpha^2)^2}{8\alpha^2}\cos 2\alpha kd - \frac{(1+\alpha^2)^2}{8\alpha^2}\right]\left(1 + \frac{\sinh 2kt_1 - 2kt_1}{2\sinh^2 kt_1}\right)$$

$$+ e^{-2k\ell}\left\{2(\alpha^2-1)kd + kg\left[\frac{(1-\alpha^2)^2}{\alpha^2} - \frac{(1+\alpha^2)^2}{\alpha^2}\cos 2\alpha kd\right] + \left(\frac{\sinh 2kt_1 - 2kt_1}{2\sinh^2 kt_1}\right)\left[\frac{(1-\alpha^2)^2}{2\alpha^2} - \frac{(1+\alpha^2)^2}{2\alpha^2}\cos 2\alpha kd\right]\right.$$

$$+ (-1)^*e^{2k\ell}\left[\frac{\alpha^4-1}{4\alpha^2} - \frac{\alpha^4-1}{4\alpha^2}\cos 2\alpha kd - \frac{\alpha^2+1}{2\alpha}\sin 2\alpha kd\right]\left(1 + \frac{\sinh 2kt_1 - 2kt_1}{2\sinh^2 kt_1}\right)$$

$$\left. + (-1)^*e^{-2k\ell}\left[\frac{1-\alpha^4}{4\alpha^2} - \frac{1-\alpha^4}{4\alpha^2}\cos 2\alpha kd - \frac{\alpha^2+1}{2\alpha}\sin 2\alpha kd\right]\left(1 - \frac{\sinh 2kt_1 - 2kt_1}{2\sinh^2 kt_1}\right)\right\}$$

0149-645X/83/0000-0187 $01.00 © 1983 IEEE

$$+ e^{-4k\ell}\left\{1 + (-1)^{*}(\alpha^2+1)kd+(-1)^{*}\ \frac{(\sinh 2kt_1-2kt_1)}{2\sin h^2 kt_1}\left(\frac{\alpha^2+1}{2\alpha}\sin 2\alpha kd + \frac{\alpha^4-1}{4\alpha^2} - \frac{\alpha^4-1}{4\alpha^2}\cos 2\alpha kd\right)\right.$$

$$+ (-1)^{*}kg\left(\frac{1+\alpha^2}{\alpha}\sin 2\alpha kd + \frac{1-\alpha^4}{2\alpha^2}\cos 2\alpha kd - \frac{1-\alpha^4}{2\alpha^2}\right) \qquad (6)$$

$$+ e^{2kg}\left(1 + \frac{\sinh 2kt_1-2kt_1}{2\sinh^2 kt_1}\right)\left[\frac{(1+\alpha^2)^2}{8\alpha^2} - \frac{(1+\alpha^2)^2}{8\alpha^2}\cos 2\alpha kd\right]$$

$$\left. + e^{-2kg}\left(1 - \frac{\sinh 2kt_1-2kt_1}{2\sinh^2 kt_1}\right)\left[\frac{1-\alpha^2}{2\alpha}\sin 2\alpha kd - \frac{(1+\alpha^2)^2}{8\alpha^2} - \frac{4\alpha^2-(1-\alpha^2)^2}{8\alpha^2}\cos 2\alpha kd\right]\right\}$$

In Eq. (6) k is positive and * = 0 for forward waves and * = +1 for backward waves. When g = 0, the above reduces to the value obtained previously[4]. η denotes meander line or parallel grating, $\tilde{J}(k)$ is the Fourier transform for the uniform current and N is the number of strip lines. The radiation reactance is then found by numerically evaluating a Hilbert transform[5], completing the radiation impedance.

Insertion Loss

Now, the insertion loss as defined and measured by commercial network analyzers such as the HP8410B Microwave Network analyzer, can be obtained with the help of Fig. 2. An MSW wave, launched by an input transducer and which reaches an output transducer is indicated by k in Fig. 2a. Transducer electrical terminals through which total transducer current flows are denoted by B and D. The power carried by the wave is represented by the electrical power dissipated in $R_m^{(+)}$. Here, we assume short connections between source and transducer terminals so that in Fig. 2b terminals A and C are connected, respectively, to terminals B and D. Insertion loss for the input transducer is defined as,

$$I.L. = -10 \log_{10} TE \qquad (7)$$

where transmission efficiency, TE, is given by

$$TE = \frac{\text{Power delivered to } R_m^{(+)}}{\text{Maximum power available}} \qquad (8)$$

From Fig. 2b. power delivered to $R_m^{(+)}$ is (1/2) $R_m^{(+)}|I|^2$ with $I=V/(R_m^{(+)}+R_m^{(-)}+R_g+jX_m)$ and $Z_g = R_g$. Maximum power available from source V, source impedance is R_g, occurs when everything to the right of terminals A and C in Fig. 2b is replaced by resistance R_g. Maximum power available is then (1/2) $R_g|I'|^2$ with $I'=V/(2R_g)$.

When the preceeding power expressions are substituted into Equations (7) and (8) insertion loss for one transducer is obtained. Assuming reciprocal coupling efficiency between electromagnetic system and MSW, TE is squared and so the total insertion loss for a pair of transducers is twice that given by Eq. (7).

$$I.L.(\pm) = 20 \log\left[\frac{(R_g + R_m)^2 + X_m^2}{4R_gR_m^{(\pm)}}\right] \qquad (9)$$

This insertion loss is identical with S_{21} in dB, the transmission loss measured by the network analyzer. Propagation loss can be included by adding a term $-76.4\ (\Delta H)\ T_g$ to Eq. (9), where T_g = group delay in microseconds and ΔH is full linewidth in oersteds. In this two terminal model ground plane effects are contained in the parameters R_m and X_m.

In Figure 3 we obtain insertion loss for forward volume waves from the two terminal model both for no gap g and for a gap g = 25 μ m. In Figure 4 we obtain insertion loss for backward volume waves for a single element both from the two terminal model and the microstrip model. In Figure 5 the same quantities are obtained for a four element parallel grating. In each of the above calculations the fundamental mode only is considered.

Conclusion

From the results presented in Figures 3-5 we see that the insertion loss obtained from the two models under discussion are in very good agreement and that the inclusion of a gap between the YIG and the transducer is significant in that the bandwidth is narrowed appreciably with increased gap. An advantage of the two terminal model is that fewer input parameters are required to calculate insertion loss while an advantage of the microstrip model is that microstrip input impedance is found naturally.

References

1. Wu, H.J., Smith, C.V., Collins, C.V. and Owens, J.M., "Bandpass Filtering with Multibar Magnetostatic surface Wave Microstrip Transducers", Electronic Letters 13 (No. 20); 1977.

2. Ganguly, A.K. and Webb, D.C.: "Microstrip Excitation of Magnetostatic Surface Waves: Theory and Experiment"; IEEE Transactions on Microwave Theory and Techniques, 1975.

3. I.J. Weinberg and J.C. Sethares, Magnetostatic Wave Transducers with Variable Coupling", RADC-TR-78-205, 1978. (AD-A063880)

4. I.J. Weinberg, "Insertion Loss for Magnetostatic Volume Waves", IEEE Transactions on Magnetics, 1982.

5. J.M. Owens and C.V. Smith; "Interaction of Magnetostatic Waves with Periodic Reflecting Structures", EMDERL 1979-AFOSR-1; 1979.

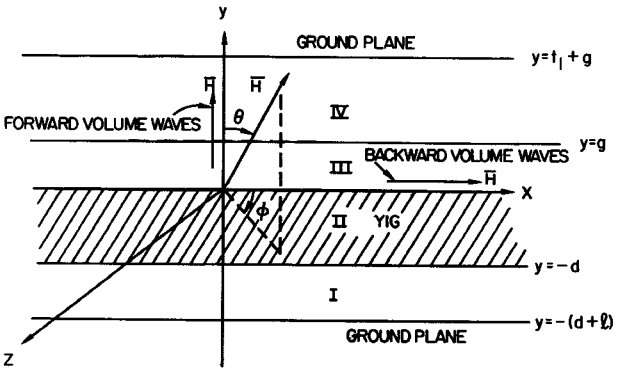

Fig. 1. Transducer geometry.

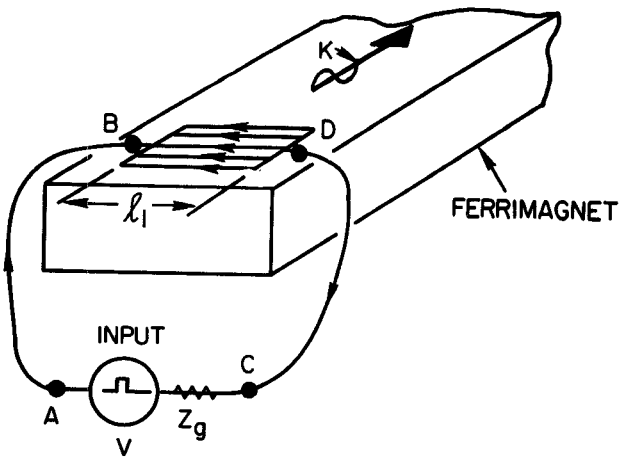

Fig. 2a. Single multielement grating transducer showing electrical and source terminals.

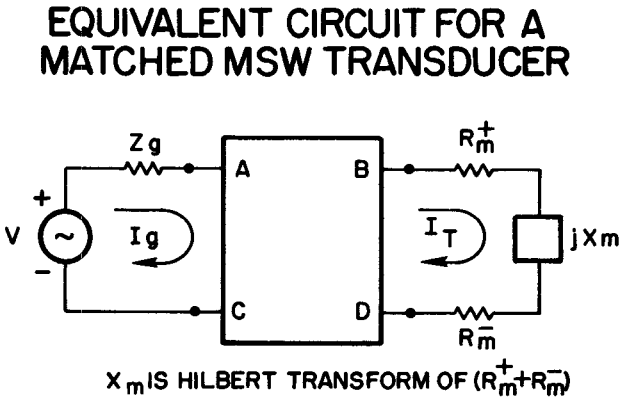

Fig. 2b. An equivalent electrical circuit for a single MSW transducer.

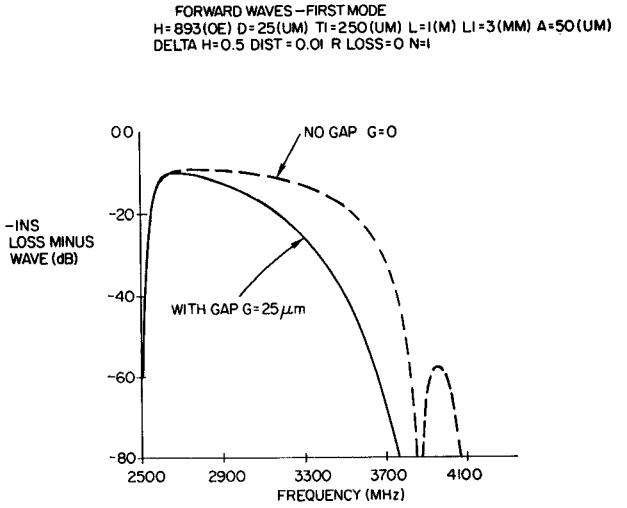

Fig. 3. Forward volume waves insertion loss - without gap and with gap.

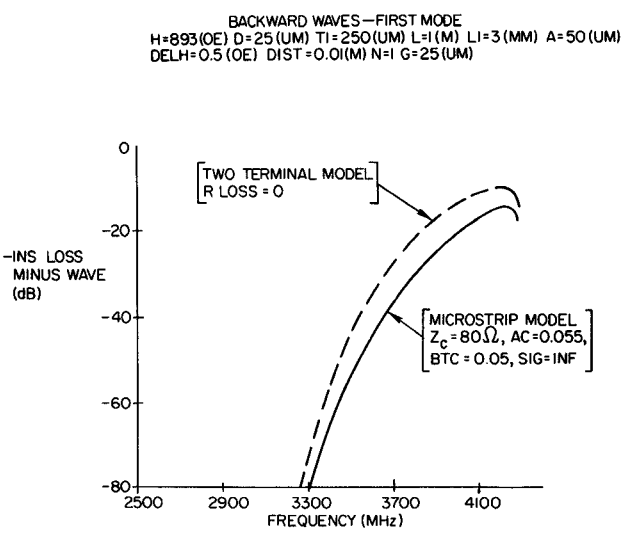

Fig. 4. Backward volume waves insertion loss for one element - two terminal and microstrip models.

PARALLEL GRATING-BACKWARD WAVES-FIRST MODE
H=893(OE) D=25(UM) T1=250(UM) L=1(M) L1=3(MM) A=50(UM) P=300(UM)
DELTA H=.5(OE) DIST.=.01(M) R LOSS=0 N=4 G=25(UM)

PARALLEL GRATING-BACKWARD WAVES-FIRST MODE-MICROSTRIP MODEL
H=893(OE) D=25(UM) T1=250(UM) L=1(M) L1=3(MM) A=50(UM) P=300(UM)
DELH=.5(OE) DIST=.01(M) N=4 G=25(UM) ZC= 80 AC=.055 BTC=.05 SIG=INF

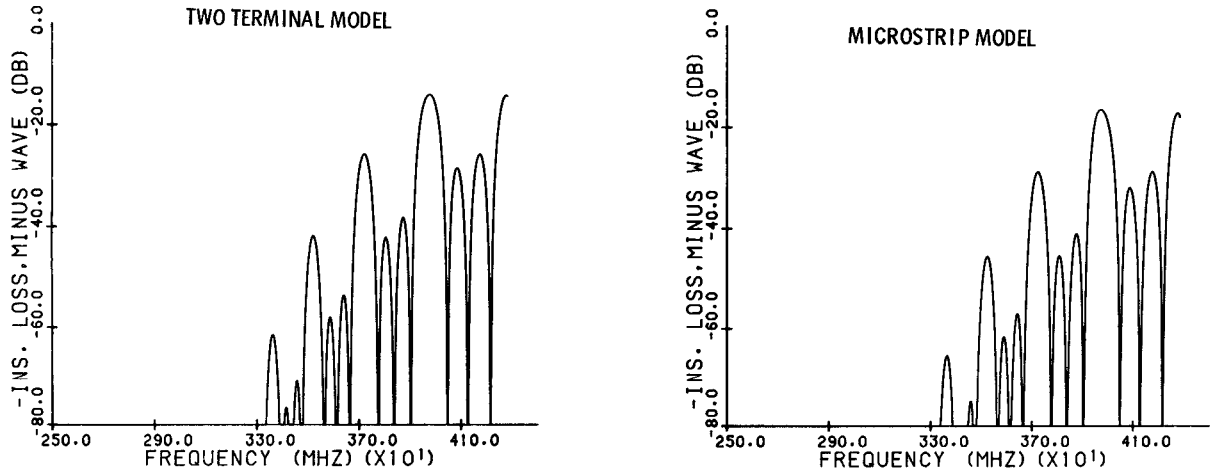

Fig. 5. Backward volume wave insertion loss - four element parallel grating - two terminal and microstrip models.